International Journal of Information Retrieval Research
Volume 12 • Issue 1

Deep Learning Model for Enhanced Crop Identification From Landsat 8 Images

Sucithra B., Anna University, Chennai, India
Angelin Gladston, Anna University, Chennai, India*

ABSTRACT

Deep learning is a powerful state-of-the-art technique for image processing, including remote sensing images. This paper describes a multilevel deep learning based crop type identification system that targets land cover and crop type classification from multi-temporal multisource satellite imagery. The proposed crop type identification is based on unsupervised neural network that is used for optical imagery segmentation and missing data restoration due to clouds and shadows, and an ensemble of supervised neural networks. The main part of this multilayer deep network with self-organizing maps and atmospheric correction is an ensemble of CNNs. The proposed system is applied for crop identification using Landsat-8 time-series and implemented with different sized vector data, parcel boundary. Aided with self-organizing maps and atmospheric correction for pre-processing doing both pixel-based and parcel-based analysis, this proposed crop type identification system allowed the authors to achieve the overall classification accuracy of nearly 95% for three different time periods.

KEYWORDS

Atmospheric Correction, Deep Learning, Landsat-8 Images, Multilayer Perceptron, Self-Organizing Maps

1. INTRODUCTION

Landsat data have become exceedingly integrated into Earth observation and monitoring applications, particularly within the last decade. This recent increase is due in part to Landsat's free and global coverage; when Landsat data became freely available in 2009, the USGS saw a 50-fold annual increase in image downloads. The Landsat program's ever-expanding image archive is an invaluable data set for ecological monitoring, change detection, and biodiversity conservation. Before these data can be used for certain ecological analyses, they must be preprocessed to account for sensor, solar, atmospheric, and topographic effects (Fangming et al, 2021). However, each preparation step further alters the data from their original values, increasing the potential to introduce error. Determining the appropriate level of preprocessing is a significant barrier to non-remote sensing scientists who lack expertise in the numerous and constantly changing techniques necessary to preprocess these data. This difficulty is exacerbated by preprocessing approaches that are similar but distinct, each with numerous possible workflows that analysts must navigate.

A comprehensive study on the state-of-the-art supervised pixel-based methods for land cover mapping was performed by Khatami et al (2016). They found that support vector machine (SVM) was the most efficient for most applications with an overall accuracy (OA) of about 75%. The second method with approximately the same efficiency (74% of OA) was a neural network (NN)-based

DOI: 10.4018/IJIRR.298648 *Corresponding Author

classifier. In that study,classification was done only for a single date image. At the same time, SVM is too much resource consuming to be used for big data applications and large area classification problems. Another popular approach in the RS domain is the random forest (RF)-based approach by P. O. Gislason et al (2006). However, multiple features should be engineered to feed the RF classifier for the efficient use.Over the past few years, the most popular and efficient approaches for multisensor and multitemporal land cover classification are ensemble-based by M. Han et al (2012), X. Huang et al (2013), M. S. Lavreniuk et al (2016) and N. Kussul et al (2016) and deep learning (DL) by Y. Gu et al (2014), S. Du et al (2016) I. Butko et al (2016), and M. Lavrenyuk et al (2015). M. Huang et al (2016), Y. LeCun et al (2006), H. Ishikawa et al (2015) used these techniques to outperform the SVM. DL is a powerful machine learning methodology for solving a wide range of tasks arising in image processing, computer vision, signal processing, and natural language processing implemented by G. Hinton (2015). The main idea is to simulate the human vision to deal with big data problem, use all the data available and provide the semantic information at the output. Plenty of models, frameworks and benchmark databases of reference imagery are available for image classification domain.

Over past years, more and more studies have been using DL for processing of RS imagery by L. Zhang et al (2015) and F. Zhang et al (2016). DL proved to be efficient for processing both optial (hyperspectral and multispectral imagery) and radar images, in extracting different land cover types such as road extraction, buildings extraction G. E. Hinton et al (2010), F. Chen et al (2015). In terms of particular DL architectures, convolutional NNs (CNNs), deep autoencoders, deep belief networks, and recurrent NN with long short-term memory model have already been explored for RS tasks by X. Jia et al (2015), Q. Li et al (2016) and L.Mou et al (2016). It should be noted that most studies with DL for RS utilize a single date image for classification purposes, e.g., land cover or object detection. However, multitemporal images are usually required to reliably identify specific land cover classes such as crop types.

In this paper, a Crop Identification System is implemented using Deep Learning in the region named Kyiv, Ukraine. This crop identification system contains modules like Data Collection, Generation of Ground truth data, Preprocessing, Supervised Classification and Geospatial Analysis. Techniques like Self Organizing Maps algorithm(SOM) refered in Gregoire Mercier et al (2010), Atmospheric Correction algorithm referred in Paul H. Evangelista et al (2017), Pixel based and Parcel based algorithms referredinYu. Shelestov et al (2016). Landsat-8 scene images are collected form the USGS and the ground truth data are generated using tools like ENVI/ArcGIS Pro.SOM and Atmospheric Correction algorithm are used for preprocessing of the satellite images. Pixel and Parcel based algorithms are used for supervised classification which are implemented on a committee of Mulilayer Perceptrons (MLPs). In Parcel based algorithm, different sizes are taken for the parcel boundaries (field boundary/ vector data) of each crop type and are implemented. Four different sizes such as 5*5, 10*10, 15*15 and 17*17 pixels are considered as the parcel boundaries.

The crop mapping based on analysis of remote sensing (RS) observations has been a critical requirement for crop monitoring and estimation of biophysical and biochemical parameters, such as yield, water demand, and damage assessment. The main contribution in this work of crop identification system is to find the different crop types or varieties or crop patterns cultivated in regions of Kyiv,Ukraine. First, to introduce new crop mapping approaches for various crops at local and regional scales through adoption of clustering, phenology, decision-tree, parcel-based, knowledge-based, multitemporal, and machine/deep learning techniques. Then the main problems such as the vegetation phenology shift due to altitudinal and latitudinal changes or the inter annual variations in climate conditions. Finally, the different vegetation growth in different fields due to the fertility of the soil, water availability, agricultural management skills, and some other reasons.For example, in double cropping systems, differentcombinations of crops are cultivated.

The rest of the paperis organized as follows: Section 2 summarizes the literature survey and the related work on the crop identification, Section3 describes the detailed design of the proposed crop identification system elaborating thecontribution for thecrop identification. Section 4 presents the

experimental setupand the implementation details.Section 5 discusses the experimental result analysis using various evaluation metrics andthenconcludes the work.

2. LITERATURE SURVEY

This section summarises the various related works that has been carried out in crop identification. The works carried out under Geospatial intelligence and data fusion techniques for land cover classification, Gradient boosting random convolutional network framework, Restricted Boltzmann machine (RBM) for hyperspectral data and Random Forests for land cover classification are presented in the following sub sections.

2.1 Geospatial Intelligence And Data Fusion Techniques Forland Cover Classification

M. Lavrenyuk et al (2015) addressed the main scientific challenges for geospatial intelligence problem solving are geospatial data fusion and correct interpretation of geospatial information. To address for big data satellite monitoring problems, the novel approach was proposedby Soheil Radiom et al (2018), based on combination of three machine learning paradigms for geospatial information analysis: big data segmentation, neural network classification and data fusion. Data fusion is performed at the pixel and at the decision making levels. During preprocessing stage, Landsat-4/5/7 and Landsat 8 scenes were merged to multichannel format for each path, row and date. The cloudy pixels from timeseries of images are restored using self-organizing Kohonen maps and after provide classification based on the time-series of restored images available for the certain year and required area. Classification was done by using an ensemble of neural networks (MLPs).

2.2 Gradient Boosting Random Convolutional Network Framework

L. Zhang et al (2016) proposed SRSCNN in which patches with a random scale are cropped from the image, and patch stretching is applied, which simulates the object scale variation to ensure that the CNN learns robust features from the remote sensing images. The random spatial scale stretching strategy. In SRSCNN, random spatial scale stretching was proposed to solve the problem of the dramatic scale variation of objects in the scene. Some objects such as airplanes and storage tanks are very important in remote sensing image scene classification. The object scale variation lead to weak feature representation for some scenes, which in turn lead to wrong classification. The assumption of the object scale variation satisfied a uniform or a Gaussian distribution and the strategy of cropping patches with a random scale following a certain distribution was applied to simulate the object variation in the scene, that forced the model to extract features that are robust to scale variation.

The robust scene classification strategy was implemented to fuse the information from different-scale patches with different locations in the image,. SRSCNN wsa applied on multiple views of one image andwere fused. The image was classified multiple times and its label were decided by voting. Then, VGGNet and GoogLeNet, used a large set of crops of multiple scales. However, unlike GoogLeNet, where only four scales ware applied in the test phase, more continuous scales ware adopted. Patches with a random position and scale ware cropped and then stretched to a fixed scale to be classified by the trained CNN model. Finally, the whole image's label was decided by selecting the label that occured the most.

2.3 Restricted Boltzmann Machine (RBM) for Hyperspectral Data

X. Jia et al (2015), investigated the characteristic of restricted Boltzmann machine (RBM) to indicate the validity for hyperspectral data classification. Reconstruction of Spectral Curves With Hidden Unitswere used. The quality of FE was examined by checking the quality of the reconstructed spectral curve. Single-layer RBMs were used with different numbers of hidden units (10, 50, 100, 150, and 200) and were trained on Indian Pines data. After the single-layer RBM learnt with hundreds of iterating

epochs, the reconstruction was computed with the hidden units. The reconstruction owned the same dimensionality with the original curve. The reconstructions were operated by RBMs. The signal-to-noise ratio (SNR) was computed with a condition that the difference between the original and the reconstruction data should be regarded as noise. If the hidden units contained enough information of the input data, the reconstruction would be good. So, RBM was considerde as an effective FE method for hyperspectral data.

RBM's Filter Characteristics: The hyperspectral data had N bands, and RBM had N input neurons and H hidden neurons. The input-to-hidden layer of an RBM was fully connected, so that every single hidden unit had its connections to every input neuron. For each hidden unit, it had N connection weights. The N connection weights were viewed as a filter, the content of certain wavelengths from input were filtered, and exaggerated the others. So, an RBM with H hidden units could be viewed as H filters. The filters wrer made visible and the N connection weights were horizontally folded to form a matrix M. The matrix M had N entries and for the whole network, there were H matrixes. Each matrix M was shown as a two-dimensional gray image and the intensities of N entries are accessed as the connection weights. The interested characteristics for those filters were observed. The filters after RBMs' learning acquired on Indian Pines and Pavia data sets were implemented by Alexandros-Stavros Iliopoulos, Tiancheng Liu, Xiaobai Sun (2015).

2.4 Random Forests For Land Cover Classification

P. O. Gislason, J. A. Benediktsson, and J. R. Sveinsson (2006), proposed Random Forest for ensemble methods using tree-type classifiers {h(x,Hk), k = 1,..., } where the {Hk} are independent identically distributed random vectors and x is an input pattern In training, the Random Forest algorithm created multiple CART-like trees, each trained on a bootstrapped sample of the original training data, and searched across a randomly selected subset of the input variables to determine a split (for each node). For classification, each tree in the Random Forest casted a unit vote for the most popular class at input x. The output of the classifier was determined by a majority vote of the trees. The number of variables was a user-defined parameter (often said to be the only adjustable parameter in Random Forest), but the algorithm was not sensitive to it. Often, a blindly selected value was set to the square root of the number of inputs.

By limiting the number of variables for a split, the computational complexity of the algorithm was reduced, and the correlation between trees was also decreased. Finally, the trees in Random Forests were not pruned, further reducing the computational load. As a result, the Random Forest algorithm ccould handle high dimensional data and use a large number of trees in the ensemble. This combined with the fact that the random selection of variables for a split seeked to minimize the correlation between the trees in the ensemble, results in error rates that had been compared to those of AdaBoost, while being computationally much lighter. As each tree is only using a portion of the input variables in a Random Forest, the algorithm is considerably lighter than conventional bagging with a comparable tree-type classifier.

In summary, when going for large scale crop mapping using available multitemporal satellite imagery, the following can be taken into consideration while using deep learning. The pixels of anygiven satellite image contain physical values. To mention, each pixel of the optical imagery contains spectral reflectance values in multiple spectral bands, and can be contaminated by the presence of clouds and shadows.Each pixel of the spaceborne SAR imagery being characterized by backscatter intensity and phase in multiple polarizations. Hence, in this crop identification system, a multilayer deep network with Self Organizing maps and atmospheric correctionare used for the classification of given multitemporal RS images both pixel and parcel based is proposed. The main part of this multilayer deep network with Self Organizing maps and atmospheric correction is an ensemble of CNNs. The proposed system is applied for crop identification using Landsat-8 time-series and implemented with different sized vector data, parcel boundary.

3. EXPERIMENTALDESIGN

This section elaborated the design details of this proposed crop identification system, which is a multilayer deep network with Self Organizing maps and atmospheric correction for the classification of given multitemporal RS images both pixel and parcel based. The following sub sections present in detail the overall crop identification system, the way Self Organizing maps and atmospheric correction are used and the various steps involved in detail.

3.1 Pre-Processing

Self Organizing maps algorithm and Atmospheric Correction algorithm are used for preprocessing of the satellite images.

3.1.1 Self Organizing Maps

Self Organizing maps algorithm(SOM) is used forthe restoration of missing data in the time-series of satellite imagery. The reason for the missing data may be the presence of clouds, shadows or smoke in the satellite image. The exact croppixel values cannot be extracted, if the satellite image has clouds, shadows or smoke. Thus SOMs can be trained for the spectral band images utilizingthe non-missing values.Missing values can thus be restored through by substituting input sample's missing components with neuron's weight coefficients.

3.1.2 Atmospheric Correction

The energy that is captured by Landsat sensors is influenced by the Earth's atmosphere. These effects could include scattering and absorption due to interactions with atmospheric particles namely, gases, water vapor, and aerosols. Atmospheric correction is used to handle these effects. However, some atmospheric effects are highly variable and thus they can be difficult to correct in Landsat imagery.

While it is not always necessary to atmospherically correct Landsat data to surface values, there are instances where this level of correction is needed. In general, absolute atmospheric corrections is implemented using the Digital numbers(DN), Reflectance values andRadiance valuesof the satellite image. The techniques used for this algorithm are extracting the Digital numbers(DN) from the satellite image, obtaining the satellite brightness temperature(SatBT), Top Of Atmosphere(TOA) and Surface Reflectance.TOA values are calculated. The NDVI values are achieved by utilizing the DN, SatBT, TOA values.

All atmospheric correction methods have associated assumptions about the target and the nature of the atmospheric particles or missivity (for land surface temperature). There are numerous atmospheric correction methods available, ranging from simple approaches that use only within-image information such as dark object subtraction (Chavez 1988), to more complex and data-intensive approaches such as the method used for the Landsat Ecosystem Disturbance Adaptive Processing System (LEDAPS) products (Masek et al. 2006).

3.1.3 Pixel Based Algorithm And Parcel Based Algorithm

Self-organizing maps are applied to restore missing pixel values in the time series of optical satellite imagery. Then, a supervised classification is performed to classify multitemporal satellite images. For this, a committee of neural networks, in particular multi-layer perceptrons, is utilized to improve the performance of individual classifiers. The MLP classifier has a hyperbolic tangent activation function for neurons in the hidden layer and logistic activation function in the output layer. The committee is formed using four MLPs with different number of hidden neurons (10, 20, 30, and 40) trained on the same training data within 250 epochs.

Outputs from different MLPs are integrated using the technique of average committee. Under this technique, the average class probability over classifiers is calculated, and the class with the highest average posterior probability for the given input sample is selected. The committee of MLPs proved

to be efficient for classifying both optical and SAR multitemporal satellite images over the study area. In this work both pixel-based approach, and parcel-based approach are used.

3.2 Proposed Crop Identification System

Figure 1 shows the detailed diagram for the proposed crop identification sytem. This crop identification system contains modules like Data Collection, Generation of Ground truth data, Preprocessing, Supervised Classification and Geospatial Analysis. The Landsat-8/OLI images are given as input for preprocessing using two techniques.Self Organizing Maps algorithm(SOM) by Gregoire Mercier et al (2010) and Atmospheric Correction algorithm byPaul H. Evangelista et al (2017) are used for preprocessing.Then, the preprocessed image is classified usingsupervised classification techniques. Pixel and Parcel based algorithms are used for supervised classification which are implemented on a committee of Mulilayer Perceptrons (MLPs). In Parcel based algorithm, different sizes are taken for the parcel boundaries (field boundary/ vector data) of each crop type and are implemented. Output is a classified image indicating different regions for the crop types.The pseudocode used in the architectural design is given below.

INPUT: Landsat-8/OLI satellite images are given input
OUTPUT: Classified image indicating different regions for the crop types.

1. The Landsat-8 scene image is preprocessed using SOM algorithm and Atmospheric correction algorithm.
2. The preprocessed image is classified using supervised classification techniques.
3. Pixel based algorithm assigns each random pixel to a particular crop type and classifies the similar pixels to form regions of the different crops.
4. Parcel based algorithm uses a polygon shaped parcel boundary(field boundary) for each crop type in which the pixels in the parcel boundary are assigned to a particular crop type and are classified to form regions.
6. The classified image with different crop type regions is obtained as output.

Figure 1. Overall crop identification system diagram

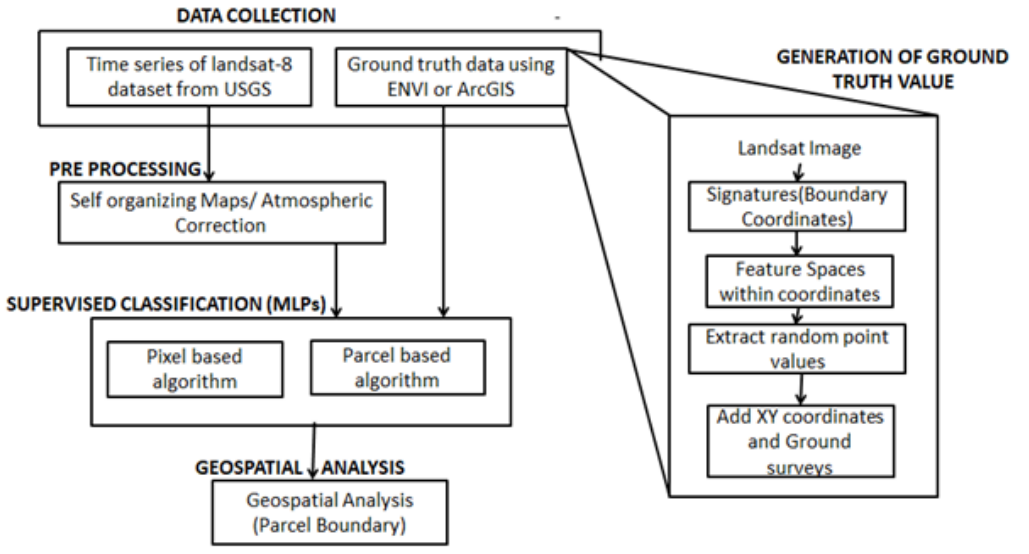

The major steps involved in this crop identification system are as follows: First, collection of Time series Landsat 8 Satellite images and Ground truth value using ENVI/ ArcGIS Pro. Second, generating Ground truth value using ENVI ArcGIS. Third, satellite image preprocessing using Atmospheric Correction and SOM Algorithm. Fourth, supervised classification using MLPs using Pixel based algorithm and Parcel based algorithm and finally performing geospatial analysis based on parcel boundary.

3.2.1 Image preprocessing using som algorithm

Figure 2. Satellite image preprocessing using SOM algorithm

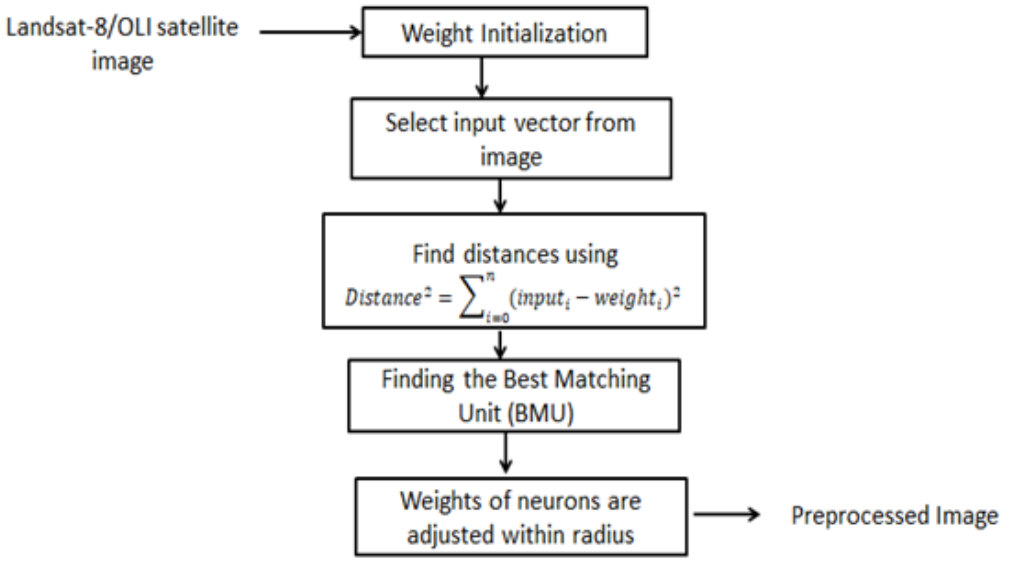

Figure 2 shows Satellite image preprocessing using SOM algorithm.The Landsat-8/OLI images are given as input and preprocessed images are returned as output. The pseudocode for this module is given below:

INPUT: Landsat-8/OLI Satellite image.
OUTPUT: Preprocessed image

1. Weight initialization
2. The input vector is selected from the dataset and used as an input for the network
3. BMU(Best Matching Unit)) is calculated:

$$Distance^2 = \sum_{i=0}^{n} \left(input_i - weight_i\right)^2 \tag{3.1}$$

4. The radius of neighbors that will be updated

$$\text{weight } (t+1) = \text{weight}(t) + \Theta(t)\, L(t)\, (\text{input}(t) - \text{weight}(t)) \tag{3.2}$$

5. Steps from 2 to 5 are repeated for each input vector of the dataset

3.2.2 Image Preprocessing Using Ac Algorithm

Figure 3. Satellite image preprocessing using AC algorithm

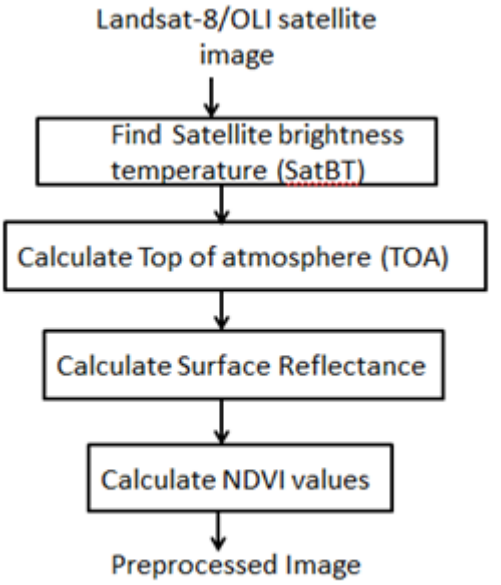

Figure 3 shows satellite image preprocessing using AC algorithm. Landsat-8 OLI images are given as input and preprocessed images are returned as output. The pseudocode for this module is given below:

INPUT: Landsat-8/OLI Satellite image.
OUTPUT: Preprocessed image

1. Using the band 10 and band 11 images, find the satellite brightness temperature (SatBT) and Top of atmosphere reflectance (TOA) value is calculated using the bands 4, 5, 10 and 11.

$$R_{TOA} = a\ *DN + b \tag{3.3}$$

2. The Surface Reflectance values are calculated using the Dark object subtraction (DOS1 & DOS2/ COST) method.
3. Finally, (NDVI) value is calculated using DN, SatBT and TOA values.

$$NDVI = \frac{\rho NIR - \rho \operatorname{Re} d}{\rho NIR + \rho \operatorname{Re} d} \tag{3.4}$$

4. The cropped image and the RGB image of the datasets are displayed.

3.2.3 Generation Of Ground Truth Values

Figure 4. Generation of ground truth value

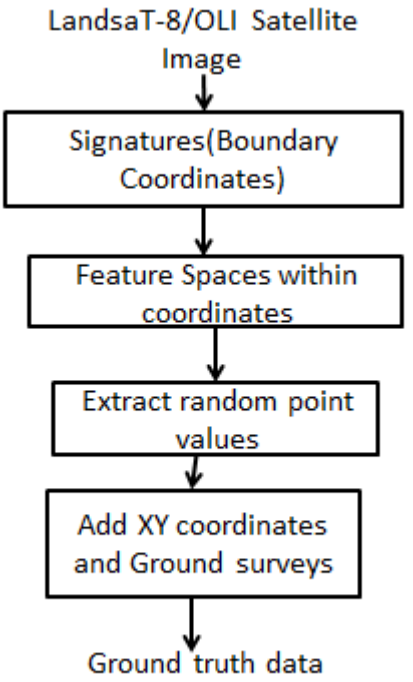

Figure 4 shows the Generation of ground truth value. The steps to collect the ground truth data using the ENVI/ ArcGIS software is mentioned as follows:

INPUT: Landsat-8/OLI Satellite image.
OUTPUT: Ground truth data

1. Each image Is from the dataset D are given as input.
2. The pixel grey value signatures are obtained from every corresponding band of the image.
3. The boundary coordinates of the desired land cover region are obtained by using the boundary box algorithm.
4. The feature spaces within the coordinates are collected.
5. The random points are extracted from the features spaces along with their XY Coordinate by using Add XY Coordinates and ground surveys information.
6. These data generated is the ground truth data.

3.2.4 Pixel Based And Parcel Based Algorithm

The Pixel and Parcel based algorithm takes the preprocessed image as input and gives the classified image as output.

1. In Pixel based algorithm, random pixels P_i from the preprocessed image are selected.

2. These individual pixels $P_i$are assigned to the a particular crop C_i and similar pixels are made to form regions.
3. In Parcel based algorithm, a set of polygon $Poly_i$shaped parcel boundary (field boundary) are selected.
4. These parcel boundaries $Poly_i$ are assigned to the crop types $C_i$and the image is classified based on the pixel values in the parcel.
5. Hence, the different regions for different crop types is identified according to the parcels by using individual pixels.

SOM and Atmospheric Correction algorithms are used for preprocessing of the satellite images. Pixel and Parcel based algorithms are used for supervised classification which are implemented on a committee of Multilayer Perceptrons (MLPs). In Parcel based algorithm, different sizes are taken for the parcel boundaries (field boundary/ vector data) of each crop type and are implemented. Four different sizes such as 5*5, 10*10, 15*15 and 17*17 pixels are considered as the parcel boundaries.

4. EXPERIMENTAL RESULTS

The crop identification system has beenimplemented and evaluated on Landsat-8/OLI scenes (Kyiv satellite images) which aredownloadedfrom U.S Geologicacal Survey (USGS) earth explorer sytem and other soures like National Aeronautics and Space Administration. By giving asatellitescene as input, the system preprocesssesthe image and returnsa classified image indicating the regions of different crop types by recognizing the secnes with itspixel values from band using SOM/ Atmospheric Correction algorithm and Pixel based and Parcel based algorithm respectively.The dataset consists of Landsat-8/OLI scene images in Kyiv region, Ukrainesatellite images were put into consideration on different date of acquisition with same path and row number. In this crop type identification system, 2 scenes with path/row coordinates 181/25 cover the test site region (Kyiv, Ukraine).

The dates of acquisition taken into consideration in this crop type identification system are November 10, October 28 and December 22. The satellite image dataset used in this crop identification system are LC08_L1TP_181025_20140910_20170419_01_T1 and the LC08_L1TP_181025_20141028_20170418_01_T1 along with their corresponding band images. Each time series date contains 9 band imagenamely, Blue (B), Cirrus (CI), Coastal (C), Coastal Aerosol (CA), Green (G), Near Infrared (NIR), Near Infrared-1 (NIR1), Near Infrared-2 (NIR2), Red (R) and Shortwave Infrared-1 (SWIR1) satellite bands.

Ground truth data were collected during ground surveys in October–December of 2017 to generate training and testing sets to train and validate the proposed classifier, respectively. Ground truth data are generated using tools like ENVI and ArcGIS Pro. Random points within a set of coordinates in the satellite image are extracted. The corresponding XY coordinates are added along with the ground surveys to the points. This data generated is the ground truth data.Figure 5shows the original Kyiv region. Figure 6 shows the classified image using parcel based algorithm in which the parcel boundary sizetaken in account is 5*5 pixels for classification.

Figure 5. Original image

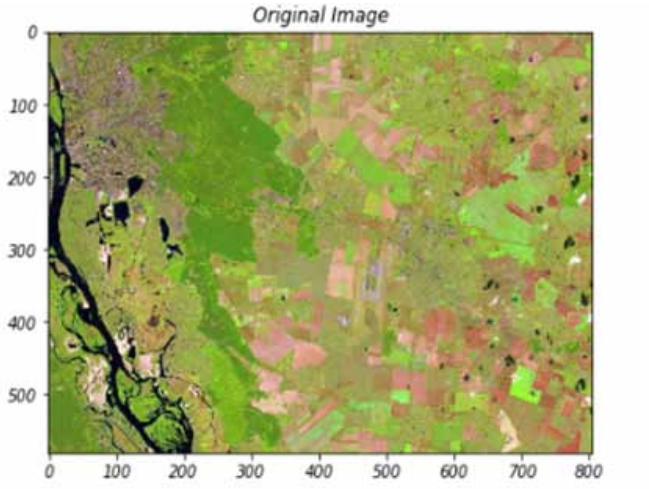

Figure 6. Parcel based algorithm implemented with 5*5 parcel size

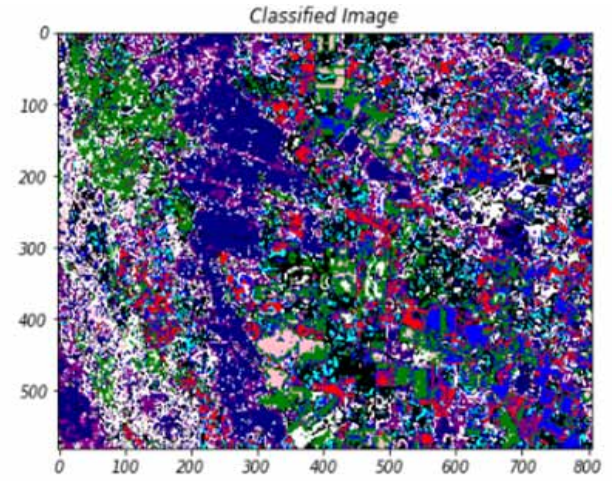

Figure 7 shows the classified image using parcel based algorithm in which the parcel boundary size taken in account is 10*10 pixels for classification. Figure 8 shows the classified image using parcel based algorithm in which the parcel boundary size taken in account is 15*15 pixels for classification.

Figure 7. Parcel based algorithm implemented with 10*10 parcel size

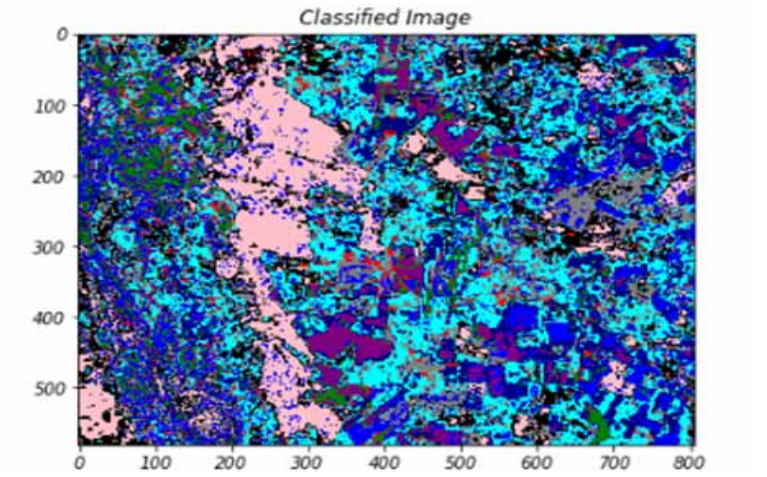

Figure 8. Parcel based algorithm implemented with 15*15 parcel size

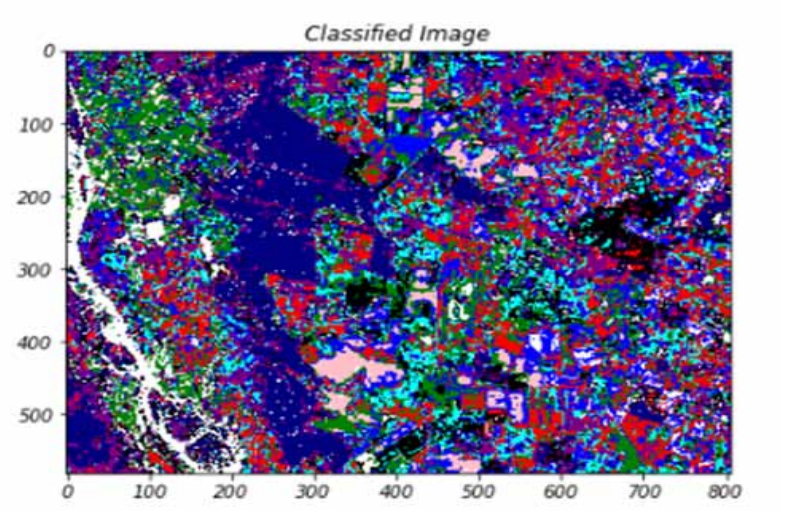

Figure 9 shows the classified image using parcel based algorithm in which the parcel boundary size taken in account is 17*17 pixels for classification. Figure 10 shows the classified image using pixel based algorithm in which the pixels are taken in account for classification.

Figure 9. Parcel based algorithm implemented with 17*17 parcel size

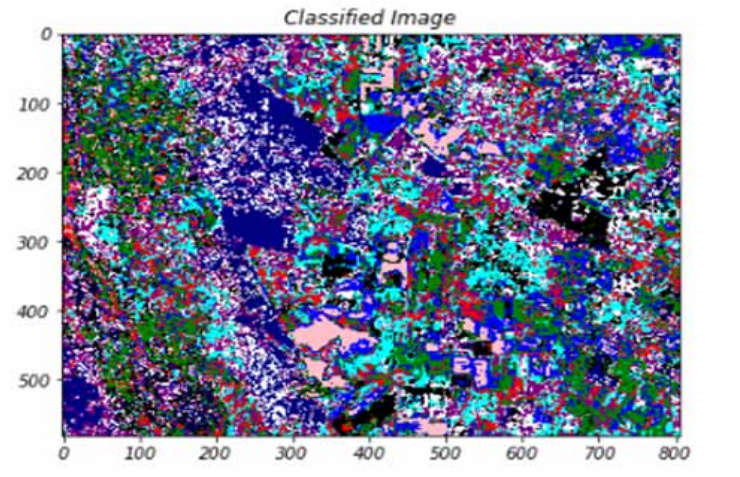

Figure 10. Pixel based algorithm implemented with only one pixel

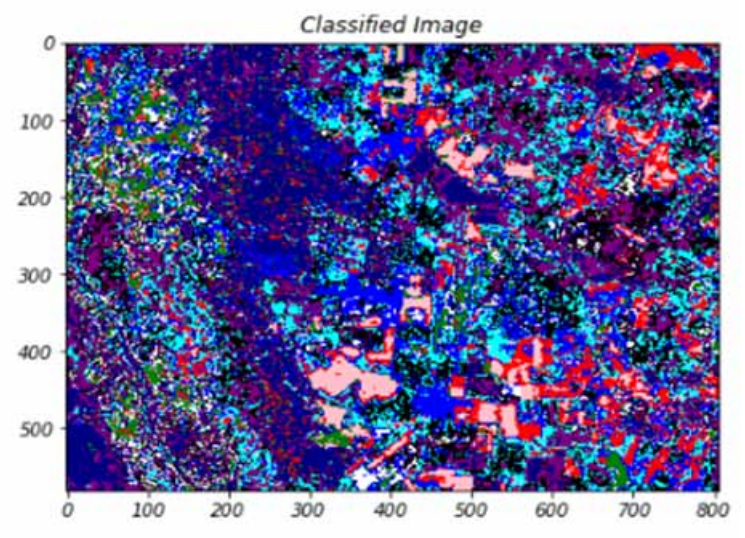

5. RESULT ANALYSIS

This section presents detailed experimental analysis on the experimental results. Table 1 shows the various test inputs, test cases used in the various steps involved. The test scenario represents the various steps of the system. Test data represents the input to the steps.

Table 1. Analysis for various Inputs

TEST CASE NO	TEST SCENARIO	TEST DATA	EXPECTED RESULT	ACTUAL RESULT
1.	B (NDVI)	Landsat 8 image (Kyiv region)	NDVI values using the DN, SatBT, TOA	NDVI values
2.	Preprocessing (Atmospheric Correction)	Landsat 8 image (Kyiv region)	Image with no missing values due to clouds/ smoke/ shadows	Image with no missing values due to clouds/ smoke/ shadows
3.	Pixel based Algorithm	Preprocessed Landsat 8 image	Different Regions of crops based on individual pixels	Different Regions of crops based on individual pixels
4.	Parcel based Algorithm Parcel size(5*5)	Preprocessed Landsat 8 image	Different Regions of crops based on parcel boundaries	Different Regions of crops based on parcel boundaries
5.	Parcel based Algorithm Parcel size(15*15)	Preprocessed Landsat 8 image	Different Regions of crops based on parcel boundaries	Different Regions of crops based on parcel boundaries
6.	Generation of Ground truth data	Landsat image in ENVI/ ArcGIS Pro	Ground truth data	Ground truth data

CASE 01

Case 01 as in Figure 11shows the NDVI values generated using MATLAB on one of the Landsat 8 image (LC08_L1TP_181025_20140910_20170419_01_T1) dataset. The zoomed image shows the NDVI generated in Kyiv region, Ukraine and the red colored area indicates the vegetation in kyiv region and may take the range values from 0.6 to 0.9.

Figure 11. Generation of NDVI values

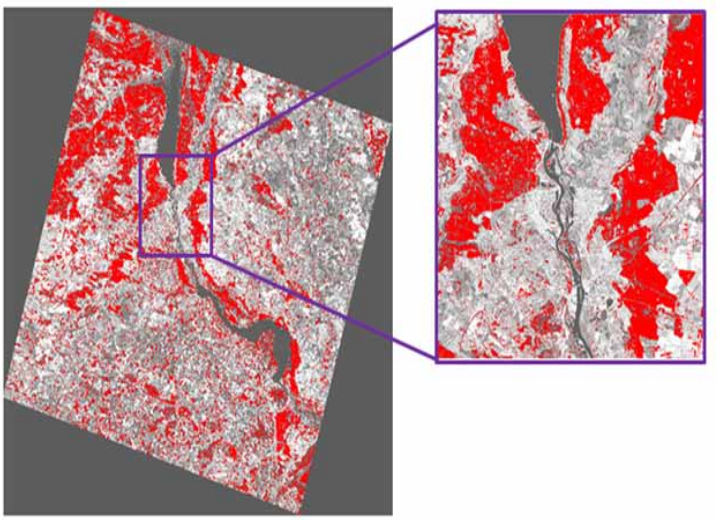

CASE 02

Case 02 as in Figure 12 shows the calculation of NDVI values using DN, TOA, DOS1, DOS2/COST while implementing Atmospherc Correction.

Figure 12. Calculation of NDVI values using DN, TOA, DOS1, DOS2/COST

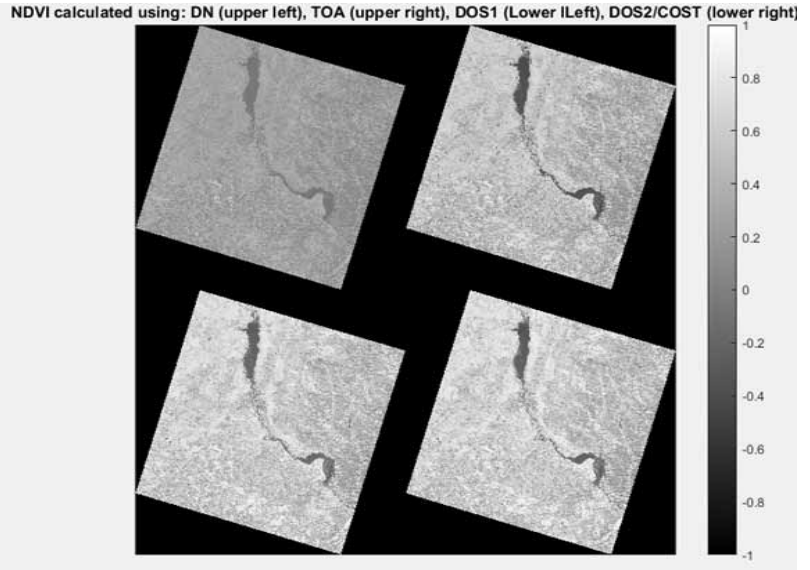

CASE 03

Case 03 in Figure 13 shows the set of parcel boundariesof size 15*15 pixels assigned the crop types. 9 set of parcel boundaries are taken from the image. Each parcel boundary contains 225 pixels. By using the ground truth data, these pixels are made to allocate to the particular crop types. Hence, based on the ground truth data, 9 parcels are assigned to 9 different crop types such as maize, winter paddy, winter raspberry, water, barley, sunflower, soy beans, forest and suger beet each holding 225 pixel data. Finally, the each crop gets their pixel data.

Figure 13. Set of parcel boundaries of size 15*15 pixels

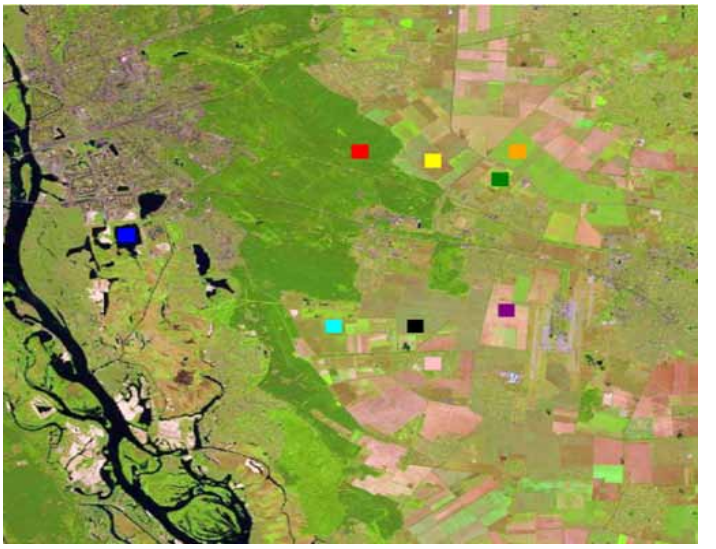

CASE 04

In Figure 14, Case 04 shows the set of parcel boundaries of size 10*10 pixels assigned to the crop types. 9 set of parcel boundaries are taken from the image. Each parcel boundary contains 100 pixels. By using the ground truth data, these pixels are made to allocate to the particular crop types. Hence, based on the ground truth data, 9 parcels are assigned to 9 different crop types such as maize, winter paddy, winter raspberry, water, barley, sunflower, soy beans, forest and suger beet each holding 100 pixel data. Finally, the each crop gets their pixel data.

Figure 14. Set of parcel boundaries of size 10*10 pixels

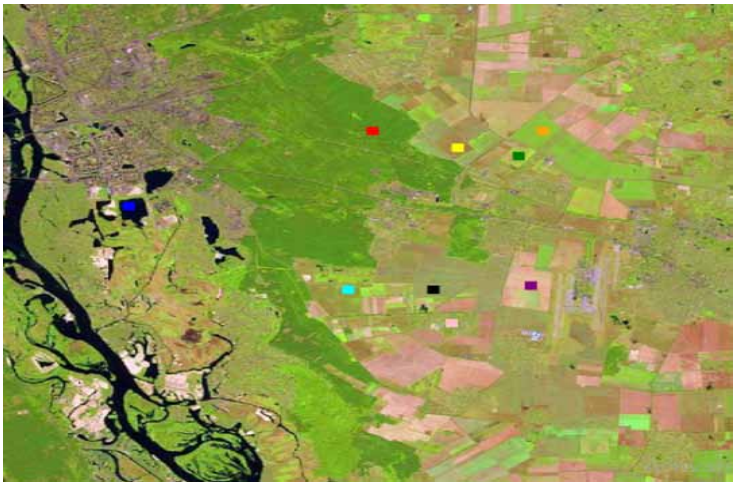

CASE 05

In Figure 15, Case05 shows the set of parcel boundaries of size 17*17 pixels assigned to the crop types. 9 set of parcel boundaries are taken from the image. Each parcel boundary contains 289 pixels. By using the ground truth data, these pixels are made to allocate to the particular crop types. Hence, based on the ground truth data, 9 parcels are assigned to 9 different crop types such as maize, winter paddy, winter raspberry, water, barley, sunflower, soy beans, forest and suger beet each holding 289 pixel data. Finally, the each crop gets their pixel data.

Figure 15. Set of parcel boundaries of size 17*17 pixels

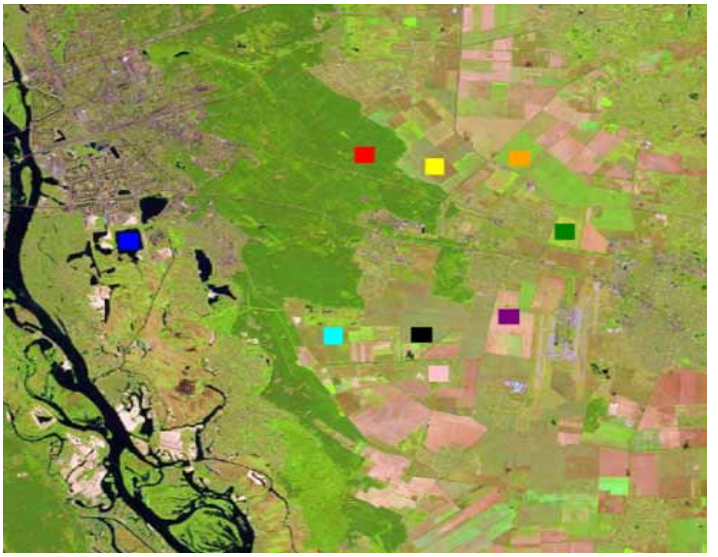

CASE 06

In Figure 16, Case 06shows the set of parcel boundaries of size 5*5 pixels assigned to the crop types.9 set of parcel boundaries are taken from the image. Each parcel boundary contains 25 pixels. By using the ground truth data, these pixels are made to allocate to the particular crop types. Hence, based on the ground truth data, 9 parcels are assigned to 9 different crop types such as maize, winter paddy, winter raspberry, water, barley, sunflower, soy beans, forest and suger beet each holding 25 pixel data. Finally, the each crop gets their pixel data.

Figure 16. Set of parcel boundaries of size 5*5 pixels

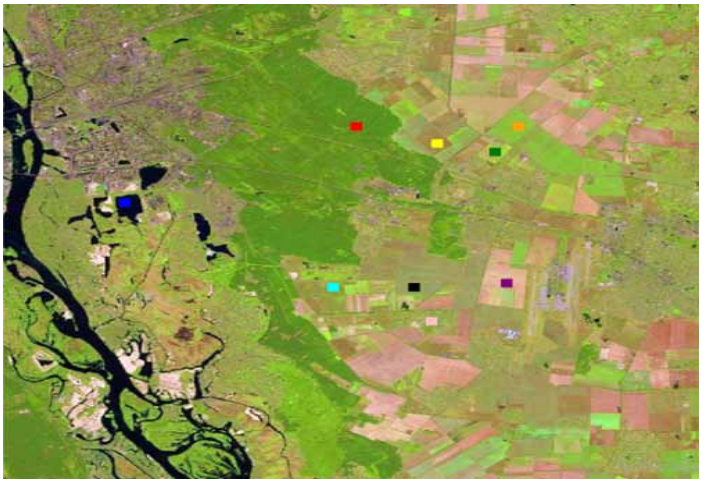

CASE 07

In Figure 17, Case07 shows the set of pixels assigned to the crop types. 9 set of parcel boundaries are taken from the image. Each parcel boundary contains only one pixel. By using the ground truth data, these pixels are made to allocate to the particular crop types. Hence, based on the ground truth data, 9 parcels are assigned to 9 different crop types such as maize, winter paddy, winter raspberry, water, barley, sunflower, soy beans, forest and suger beet each holding only one pixel data. Finally, the each crop gets their pixel data.

Figure 17. Set of 9 pixels

Figure 18 shows the ground truth data generated using ArcGIS Pro and Figure 19 shows the sample of ground truth data.

Figure 18. Generated ground truth data

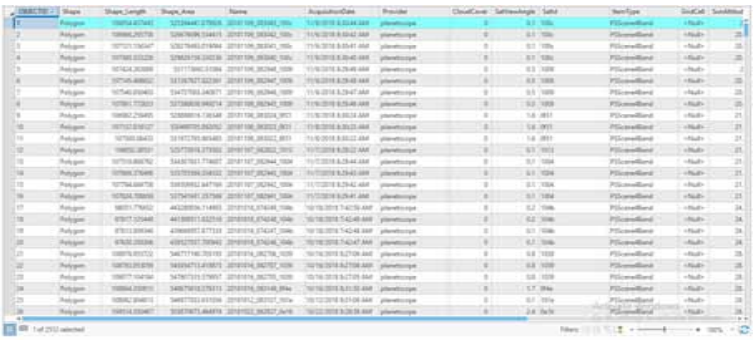

Figure 19. Sample Ground truth data

14	Polygon	107969.3758488	5357059983.334332	20181107_082843_1004	11/7/2018 8:28:43 AM	planetscope	0	0.1	1004	PSScene4Band	<Null>	21.
15	Polygon	107764.6847581	5361509832.647769	20181107_082842_1004	11/7/2018 8:28:42 AM	planetscope	0	0.1	1004	PSScene4Band	<Null>	21.
16	Polygon	107824.7086591	5373549931.357569	20181107_082841_1004	11/7/2018 8:28:41 AM	planetscope	0	0.1	1004	PSScene4Band	<Null>	21.
17	Polygon	98051.77766321	4432808556.114893	20181018_074349_104b	10/18/2018 7:43:50 AM	planetscope	0	0.2	104b	PSScene4Band	<Null>	24.
18	Polygon	97817.1254481	4415095911.622516	20181018_074348_104b	10/18/2018 7:43:49 AM	planetscope	0	0.2	104b	PSScene4Band	<Null>	24.
19	Polygon	97613.0089346	4398669857.877333	20181018_074347_104b	10/18/2018 7:43:48 AM	planetscope	0	0.1	104b	PSScene4Band	<Null>	24.
20	Polygon	97630.3503806	4395270317.709943	20181018_074346_104b	10/18/2018 7:43:47 AM	planetscope	0	0.1	104b	PSScene4Band	<Null>	24.
21	Polygon	108078.9557221	5457177190.705165	20181016_082706_1039	10/16/2018 8:27:06 AM	planetscope	0	0.8	1039	PSScene4Band	<Null>	28.
22	Polygon	108783.9533659	5459547213.418873	20181016_082707_1039	10/16/2018 8:27:08 AM	planetscope	0	0.8	1039	PSScene4Band	<Null>	28.

The Crop type identification system has been analyzed by using variousevaluation metrics,namelyaccuracy, recall, precision and f score. The important parameters for measuring these evaluation metrics are true positive, true negative, false positive and false negative. From these values Accuracy, Precision, Recall and F1 score are computed based on the equations shown.

Table 2. Evaluation Metrics

	Predicted class		
Actual Class		Class = Yes	Class = No
	Class = Yes	True Positive	False Negative
	Class = No	False Positive	True Negative

In Table 2, true positive and true negatives are the observations that are correctly predicted and therefore shown in light grey color. The goal is to minimize false positives and false negatives so they are shown in dark grey color.

Accuracy: Accuracy is the most intuitive performance measure and it is simply a ratio of correctly predicted observation to the total observations. If there is high accuracy, then the model is best. Accuracy is a great measure but only when we have symmetric datasets where values of false positive and false negatives are almost same.

$$\text{ACCURACY} = \frac{\text{TP} + \text{TN}}{\text{TP} + \text{TN} + \text{FP} + \text{FN}} \tag{1}$$

Precision: Precision is the ratio of correctly predicted positive observations to the total predicted positive observations. High precision relates to the low false positive rate.

$$\text{PRECISION} = \frac{\text{TP}}{\text{TP} + \text{FP}} \tag{2}$$

Recall (Sensitivity): Recall is the ratio of correctly predicted positive observations to the all observations in actual class.

$$\text{RECALL} = \frac{\text{TP}}{\text{TP} + \text{FN}} \tag{3}$$

F Score: F Score is the weighted average of Precision and Recall. Therefore, this score takes both false positives and false negatives into account. F1 Score is usually more useful than accuracy, especially if there is an uneven class distribution. Accuracy works best if false positives and false negatives have similar cost. If the cost of false positives and false negatives are very different, it's better to look at both Precision and Recall.

$$\text{F SCORE} = 2.\ \frac{PRECISION.\ \ RECALL}{PRECISION + RECALL} \tag{4}$$

The Accuracy obtained from various iterations by Parcel based algorithm is shown in the Figure20. "Parcel4" and "Parcel3" indicates the accuracy of iterations taken from parcel boundary of size 5*5 and 10*10 pixels respectively. Similarly, "Parcel2" and "Parcel1" indicates the accuracy for iterations taken from parcel boundary of size 15*15 and 17*17 pixels respectively.

Figure 20. Comparison of Parcel and Pixel based algorithms

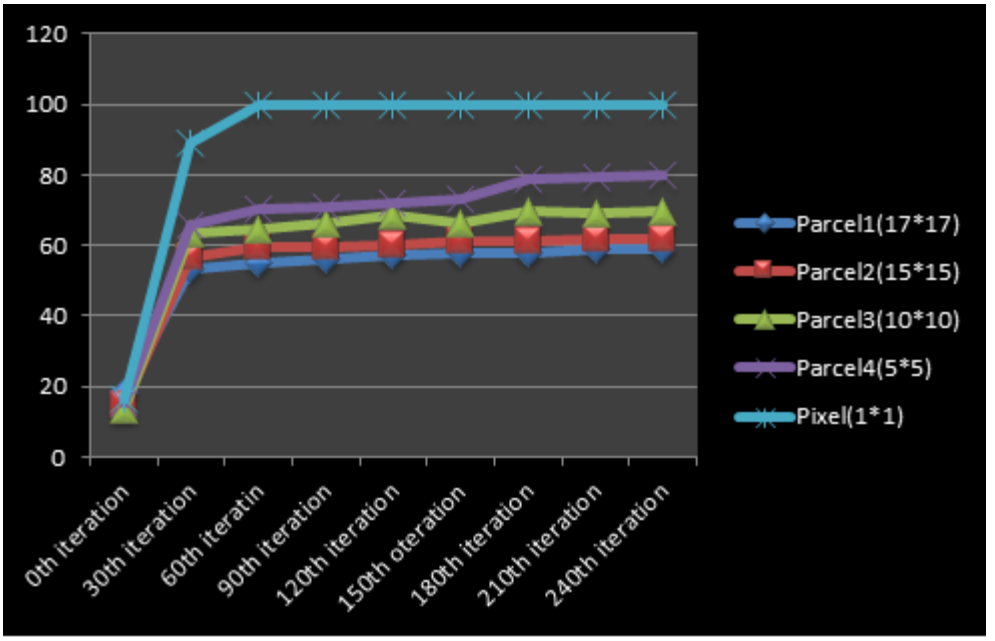

From Figure 20, we can infer that among the Parcel boundaries Parcel4 (i.e., parcel boundary of size 5*5 pixels) is accurate than any other parcel boundary sizes.While comparing with pixel and parcel based algorithms, pixel based algorithm gives accurate classification than parcel based algorithm. The classified image for Parcel4, Parcel3, Parcel3, Parcel1 and Pixel is shown in Figure 13, Figure 14, Figure 15, Figure 16 and Figure 17respectively.Figure 21 shows the comparison of Precision, Recall, F1-Score values obtained for various Parcel and Pixel based algorithms. From Figure 21, we can infer that in this crop type identification system, the Pixel based algorithm (Pixel) has high values than the Parcel based algorithms. Among the parcel based algorithms, parcel boundary with size 5*5 pixels (Parcel4) is said to have high values than the other Parcel based algorithms.

Figure 21. Comparison of Precision, Recall, F1-Score between Parcel and Pixel based algorithms

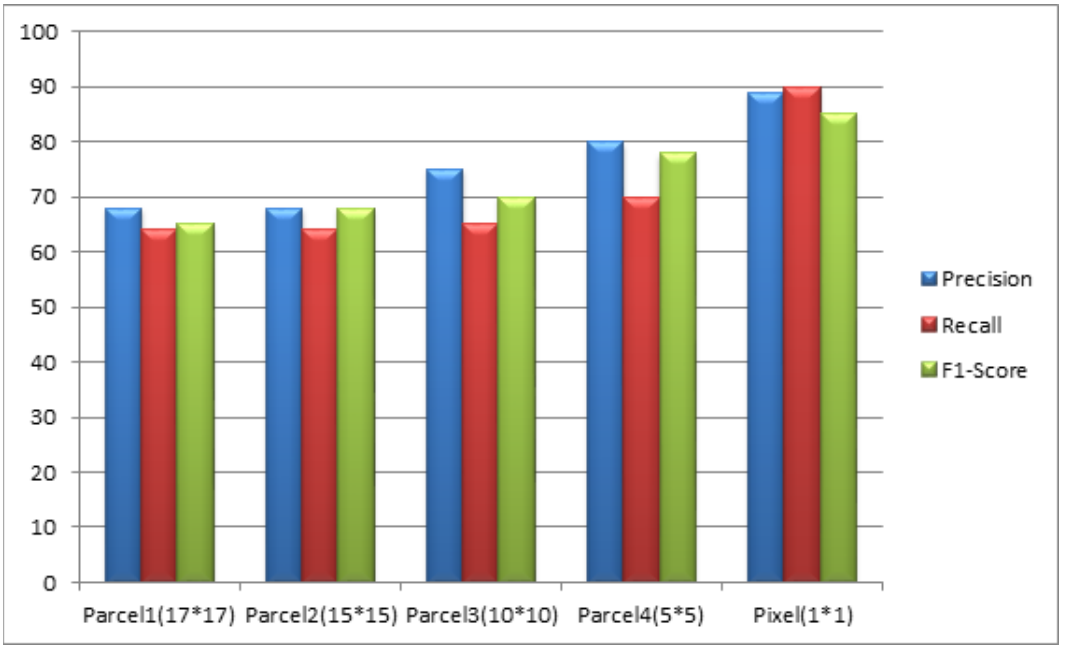

CONCLUSION

The proposed method leverages the different crop types or varieties or crop patterns cultivated in regions of Kyiv,Ukraine. The main idea of the proposed crop type identification system is the use of supervised neural networks with MLPs, aided with self organizing maps and atmospheric correctionfor pre-processing doing both pixel based and parcel based analysis. This proposed approach allowed us to achieve the overall classification accuracy of nearly 95% for three different time periods (2014 and 2017) and improve quality of maps comparing to other land cover maps available for Ukraine at 30m spatial resolution. Extensive experimental results show that the proposed algorithm outperforms the state-of-the-art methods on Landsat 8/OLI satellite images such as the LC08_L1TP_181025_20140910_20170419_01_T1 and the LC08_L1TP_181025_20141028_20170418_01_T1 and the corresponding band images for the Kyiv region in Ukraine.

FUNDING AGENCY

Publisher has waived the Open Access publishing fee.

REFERENCES

Ashourloo, D., Aghighi, H., Matkan, A. A., & Radiom, S. (2018). A Novel Automatic Method for Alfalfa Mapping Using Time Series of Landsat-8. *IEEE Journal of Selected Topics in Applied Earth Observations and Remote Sensing*, *8*(2), 70. doi:10.1109/JSTARS.2018.2874726

Chen, Y., Lin, Z., Zhao, X., Wang, G., & Gu, Y. (2014). Deep learning-based classification of hyperspectral data. *IEEE Journal of Selected Topics in Applied Earth Observations and Remote Sensing*, *7*(6), 2094–2107. doi:10.1109/JSTARS.2014.2329330

Chen, Y., Zhao, X., & Jia, X. (2015). Spectral–spatial classification of hyperspectral data based on deep belief network. *IEEE Journal of Selected Topics in Applied Earth Observations and Remote Sensing*, *8*(6), 2381–2392. doi:10.1109/JSTARS.2015.2388577

Ding, J., Chen, B., Liu, H., & Huang, M. (2016). Convolutional neural network with data augmentation for SAR target recognition. *IEEE Geoscience and Remote Sensing Letters*, *13*(3), 364–368. doi:10.1109/LGRS.2015.2513754

Geng, J., Fan, J., Wang, H., Ma, X., Li, B., & Chen, F. (2015). High-resolution SAR image classification via deep convolutional autoencoders. *IEEE Transactions on Geoscience and Remote Sensing*, *12*(11), 2351–2355. doi:10.1109/LGRS.2015.2478256

Gislason, P. O., Benediktsson, J. A., & Sveinsson, J. R. (2006). Random Forests for land cover classification. *Pattern Recognition Letters*, *27*(4), 294–300. doi:10.1016/j.patrec.2005.08.011

Han, M., Zhu, X., & Yao, W. (2012). Remote sensing image classification based on neural network ensemble algorithm. *Neurocomputing*, *78*(1), 133–138. doi:10.1016/j.neucom.2011.04.044

Huang, F. J., & LeCun, Y. (2006). Large-scale learning with SVM and convolutional for generic object categorization. *IEEE Computer Society Conference on Computer Vision and Pattern Recognition*, 284–291.

Khatami, R., Mountrakis, G., & Stehman, S. V. (2016). A meta-analysis of remote sensing research on supervised pixel-based land-cover image classification processes. *Remote Sensing of Environment*, *177*, 89–100. doi:10.1016/j.rse.2016.02.028

Kussul, N., Lavreniuk, N., Shelestov, A., Yailymov, B., & Butko, I. (2016). Land cover changes analysis based on deep machine learning technique. *Journal of Automation and Information Sciences*, *48*(5), 42–54. doi:10.1615/JAutomatInfScien.v48.i5.40

Kussul, N., Lemoine, G., Gallego, F. J., Skakun, S. V., Lavreniuk, M., & Shelestov, A. Y. (2016). Parcel-based crop classification in Ukraine using Landsat-8 data and Sentinel-1A data. *IEEE Journal of Selected Topics in Applied Earth Observations and Remote Sensing*, *9*(6), 2500–2508. doi:10.1109/JSTARS.2016.2560141

Latif & Mercier (2010). *Self-Organizing maps for processing of data with missing values and outliers: application to remote sensing images*. Academic Press.

Lavreniuk, M. S., Skakun, S. V., Shelestov, A. J., Yalimov, B. Y., Yanchevskii, S. L., Yaschuk, D. J., & Kosteckiy, A. Ì. (2016). Large-scale classification of land cover using retrospective satellite data. *Cybernetics and Systems Analysis*, *52*(1), 127–138. doi:10.1007/s10559-016-9807-4

Liang, H., & Li, Q. (2016). Hyperspectral imagery classification using sparse representations of convolutional neural network features. *Remote Sensing*, *8*(2), 99. doi:10.3390/rs8020099

Lyu, H., Lu, H., & Mou, L. (2016). Learning a transferable change rule from a recurrent neural network for land cover change detection. *Remote Sensing*, *8*(6), 506. doi:10.3390/rs8060506

Mnih, V., & Hinton, G. E. (2010). Learning to detect roads in highresolution aerial images. *Proceeding European Conference on Computer Vision*, 210–223.

Wu, F., Wu, B., Zhang, M., Zeng, H., & Tian, F. (2021). Identification of Crop Type in Crowdsourced Road View Photos with Deep Convolutional Neural Network. *Sensors (Basel)*, *2021*(21), 1165. doi:10.3390/s21041165 PMID:33562266

Young, Anderson, Chignel, Vorster, Lawrence, & Evangelista. (2017). A survival guide to Landsat preprocessing. *Concepts and Synthesis Emphasizing New Ideas to Stimulate Research in Ecology, 98*(4), 920–932.

Zhang, F., Du, B., & Zhang, L. (2015). Saliency-guided unsupervised feature learning for scene classification. *IEEE Transactions on Geoscience and Remote Sensing*, *53*(4), 2175–2184. doi:10.1109/TGRS.2014.2357078

Zhang, F., Du, B., & Zhang, L. (2016). Scene classification via a gradient boosting random convolutional network framework. *IEEE Transactions on Geoscience and Remote Sensing*, *54*(3), 1793–1802. doi:10.1109/TGRS.2015.2488681

Zhao, W., & Du, S. (2016). Learning multiscale and deep representations for classifying remotely sensed imagery. *ISPRS Journal of Photogrammetry and Remote Sensing*, *113*, 155–165. doi:10.1016/j.isprsjprs.2016.01.004

Sucithra B. is a post graduate student of the Department of Computer Science and Engineering, Anna University, Chennai. Her research interests include image processing and machine learning.

Angelin Gladston is working as Associate Professor at the Department of Computer Science and Engineering, Anna University, Chennai. Her research interests include software engineering, software testing, image processing, social network analysis and data mining.